Available online at www.sciencedirect.com
ScienceDirect
Journal of Sound and Vibration 297 (2006) 895–915
JOURNAL OF SOUND AND VIBRATION
www.elsevier.com/locate/jsvi

Drum-like silencers using magnetic forces in a pressurized cavity

Y.H. Chiu, L. Cheng*, L. Huang

Department of Mechanical Engineering, The Hong Kong Polytechnic University, Hung Hom, Kowloon, Hong Kong SAR, PR China

Received 1 August 2005; received in revised form 21 April 2006; accepted 2 May 2006
Available online 5 July 2006

Abstract

A feasibility study is carried out for utilizing magnetic force to yield a low-frequency shift of the transmission loss spectrum provided by a drum-like silencer consisting of two side-branch, rectangular cavities covered by ferromagnetic membranes. The results show that the transmission loss spectrum of the drum-like silencer is mainly controlled by the vibration of the first and second modes of the membrane. Three pairs of magnets are employed inside the cavity to promote the response of these modes. It is found that the magnetic force imposes both static and dynamic effects on the silencer. While the latter helps shift the effective region of the silencer towards lower frequencies, the former results in an increase of stiffness of the membrane which is detrimental to the operation of the silencer at low frequencies. Cavity pressurization is then proposed to neutralize the static effects of the magnetic force. A finite element model is developed to predict and optimize the performance of the proposed silencer with some of the results validated experimentally. The desired shift towards the lower frequency is validated although the silencer performance is still less than ideal due to both parametric and operational constraints of the rig.

1. Introduction

Low-frequency noise is very annoying and difficult to attenuate since most of the dissipative noise absorbers are ineffective and conventional reactive silencers are bulky. As an alternative, active noise control (ANC) is regarded as a suitable technique in low-frequency noise control [1]. However, some drawbacks related to the technique still limit its use in noise control practices. Its cost, sophistication in design and reliability are just a few key factors. For this reason, it is still necessary and desirable to extend the low-frequency limit for passive noise control.

Helmholtz resonator is commonly used in passive noise control. It consists of a neck and a cavity and produces a resonance frequency at which a very high transmission loss can be achieved within a very narrow bandwidth. In order to extend the usefulness of the device, many adaptive-passive noise control techniques have been developed [2,3]. In those techniques, the resonator neck dimensions, cavity volume, or both are adjusted according to the working condition. However, the involvement of active tuning devices inherits the cost and reliability drawbacks from ANC.

*Corresponding author. Tel.: +852 2766 6769; fax: +852 2365 4703.
E-mail address: mmlcheng@polyu.edu.hk (L. Cheng).

0022-460X/$ - see front matter © 2006 Elsevier Ltd. All rights reserved.
doi:10.1016/j.jsv.2006.05.006

To deal with these problems, Huang and Choy [4–9] proposed to use a drum-like silencer to control the duct noise from low-frequency to medium-frequency range. When a sound wave travels over the cavity-backed membrane in a duct, the sound wave in air is coupled with the flexural waves over the membrane, and the membrane compliance makes the coupled wave speed less than the speed of sound in air [4]. This represents an acoustic impedance discontinuity at a junction where the physical geometry of the duct remains unchanged. The discontinuity reflects sound, much like an expansion chamber does, and there is also acoustic scattering. If the drum-like silencer is properly designed, a large amount of the incoming sound energy can be reflected to the source, hence reducing the noise downstream. Although the performance of this type of silencer for the low-frequency duct noise is limited by the cavity stiffness, it provides a new concept for extending the effective bandwidth of the transmission loss spectrum with a compact passive device.

To overcome the cavity stiffness of drum-like silencers with shallow cavities, Huang [10] further proposed the use of magnetic force. A theoretical analysis assuming a piston-like behaviour of the membrane shows that zero impedance of the membrane type silencer may be maintained over a certain band of frequencies so that the low-frequency limit can be removed with the help of dynamic magnetic effect. As shown in Fig. 1, when a permanent magnet is separated from a ferromagnetic membrane by an air gap of d, an attractive force is generated to promote the displacement of the membrane. This attractive force increases when the membrane is drawn into the cavity, and vice versa. Given the dynamic magnetic force per unit area as $F_{\mathrm{dyn}} = B/(d+\eta)^2$, where B is the magnetic flux density and η the vibration displacement of the membrane, a magnetically induced stiffness is introduced by the magnetic force, which is proportional to $-2Bd^{-3}$ and is negative. Therefore the factor of d^{-3} provides an effective way to balance the cavity stiffness and the mechanical stiffness of the membrane.

Previous investigations, however, totally bypass issues of practical implementation with a lack of experimental support. Moreover, by assuming piston behaviour for the membrane, the effect of the static magnetic force on the membrane tension has not been considered. In fact, given a real membrane, apart from the dynamic magnetic force, a static magnetic force is also imposed on the membrane. The static magnetic force is defined as $F_{\mathrm{stat}} = B/(d+\eta_o)^2$ where η_o is the static membrane deflection. In this case, the membrane tension is increased to balance the static magnetic force and hence the mechanical stiffness of the membrane increases. Therefore the increase in the mechanical stiffness may exceed the magnitude of the negative magnet induced stiffness.

In the current study, a simplified theoretical model considering both static and dynamic effects of the magnetic force is established. This theoretical analysis shows that the performance of the proposed silencer is mainly dominated by the vibration of the first and second modes of the membrane. Therefore the low-frequency shift of the transmission loss can be achieved by properly locating three pairs of magnets in the cavity to maximize the vibration amplitudes of the first two modes.

Results show that the static magnetic effect sometimes exceeds the dynamic magnetic effect. As a result, magnetic forces shift the effective range of the drum-like silencer to higher frequencies rather than to lower frequencies. To suppress the static magnetic effect, a pressurized cavity is introduced in this study. The role of the cavity pressure is to balance the static magnetic force. Although the pressurization also increases the cavity stiffness, its effect on reducing the membrane tension far outweighs its own contribution to the cavity stiffness.

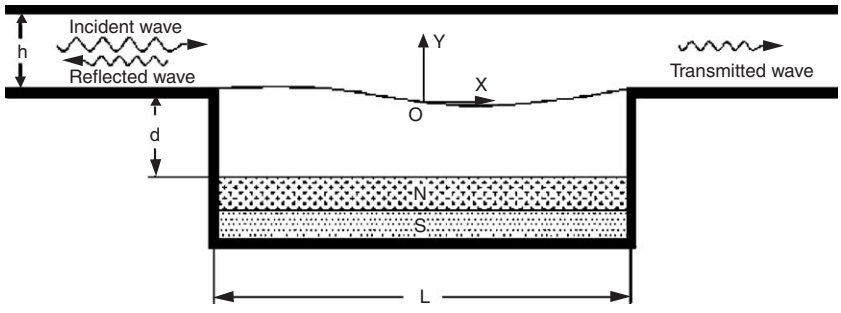

Fig. 1. Theoretical model of a drum-like silencer with magnetic force. A magnetic, tensioned membrane of length L lines part of the otherwise rigid duct wall. The cavity of depth d is equipped with a pair of permanent magnets with North and South poles as shown.

This is so because, when the membrane is flat initially, membrane tension is unable to resist transverse displacement. If the static magnetic force applied on the membrane is uniform, cavity pressure is set to $P_{cav} = F_{stat}$ and hence $\eta_o = 0$. Therefore, the membrane tension will not be increased and the dynamic magnetic effect is still effective to overcome the cavity air stiffness. In practical implementation of the magnetic force, the magnetic effect is applied on the membrane in a non-uniform way. Therefore, zero deflection of the membrane cannot be achieved everywhere even with the use of a pressurized cavity. This significantly increases the complexity of the analysis. It requires a more sophisticated model to carry out parametric optimization. To this end, a finite element (FE) model is developed to predict and to optimize the performance of the proposed silencer. This FE model fully couples the membrane vibration, acoustic pressure and the magnetic field, and is validated experimentally.

It is pertinent to mention that the present study constitutes a step forward on the development of a novel noise control device. Further investigations are certainly needed to tackle various issues regarding its practical implementation before such a device can find its applications in a number of areas such as the acoustic quietening in ventilation duct systems, tunnels and engine testing chambers, etc.

2. A theory of uniform magnetic field

This section outlines the theory of a drum-like silencer and reveals the influence of the magnetic effect on a drum-like silencer. The underlying theory is the principle of vibroacoustic coupling between a flexible membrane and the acoustic wave (see Refs. [4–9]). To simplify the theoretical analysis, it is assumed that a static magnetic force is applied on a ferromagnetic membrane by using a single large magnet while the volume occupying the cavity is ignored.

The theoretical model under investigation is shown in Fig. 1. It has a two-dimensional (2D) duct (channel) of height h lined in part by a membrane of length L and width h on the lower wall. In the subsequent theoretical modelling, the membrane is actually represented by a one-dimensional (1D) string, and the whole configuration is denoted as a 2D model as the channel is 2D in space. As a first step in modelling the magnetic effect, the 2D model is adopted instead of the three-dimensional (3D) configuration implemented in experiment. A 3D configuration for the cavity would embrace all cavity walls and the membrane becomes 2D instead of 1D (a string) in the current model. For a 2D membrane, it has four edges and they all have to be fixed on the cavity walls, which seems to differ from the current model substantially. Besides the desire to keep analysis simple at this stage, the following result from Ref. [9] provides justification for such a simplification. It was found that, when the transverse tension, T_y, vanished, the transmission loss of the drum-like silencer represented by a 3D model was identical to that of the 2D model although the membrane vibration differed. It was also found that the presence of $T_y > 0$ would be unhelpful for the silencer performance. These conclusions were validated experimentally in that study. If, in the current study, static imbalance exists and the membrane deforms before sound induced vibration occurs, the result predicted by the 2D model would differ from the reality of a 3D configuration. However, when the static balance is achieved by the method of cavity pressurization, T_y is expected to vanish and the 2D model is expected to predict the same result as a 3D model.

The membrane is fixed at the two edges at $|x| = L/2$, and is enclosed by a rigid-walled cavity of depth d, length L. The mass per unit length of the membrane is m and the tension applied on the membrane is T. The separation between the ferromagnetic membrane and the magnet is d. The static equation of the ferromagnetic membrane is

$$\nabla \cdot (T \nabla \eta_0) = \frac{\psi}{(d+\eta_0)^2}, \quad T = \begin{bmatrix} T_x & 0 \\ 0 & T_y \end{bmatrix}, \quad \nabla \eta_0 = \begin{bmatrix} \partial \eta_0 / \partial x \\ \partial \eta_0 / \partial y \end{bmatrix}, \tag{1}$$

where both the tensile stresses T and the vector $\nabla \eta_0$ should be interpreted as matrices as tension differs in x and y directions. As the membrane is fixed at two edges only, $T_y = 0$ and $\partial \eta_0 / \partial y = 0$. The stress–strain relationship of the membrane can be described as [11]

$$\varepsilon_x = \frac{\mathrm{d}u}{\mathrm{d}x} + \frac{1}{2}\left(\frac{\mathrm{d}\eta_0}{\mathrm{d}x}\right)^2 \quad \text{and} \quad E\tau\varepsilon_x = T_x - T_o, \tag{2}$$

where η_0 is the static membrane deflection, Ψ the constant magnetic function, τ the thickness of the membrane, ε_x the strain of the membrane in the x-direction, u the displacement in the x direction for a membrane element of finite length, E the Young's modulus of the membrane and T_o the initial tension applied to the stretched membrane. The derivation of Eq. (1) is shown in Appendix A. Assuming that the initial membrane tension is high enough so that the displacement in the x direction for a membrane element can be ignored, Eq. (2) can be combined to form an equation for the resultant tension in the membrane:

$$\frac{E\tau}{2}\left(\frac{\mathrm{d}\eta_0}{\mathrm{d}x}\right)^2 = T_x - T_o. \tag{3}$$

Putting Eq. (3) into Eq. (1) yields

$$\nabla\cdot\left(\frac{E\tau}{2}\left(\frac{\mathrm{d}\eta_0}{\mathrm{d}x}\right)^2\nabla\eta_0 + T_o\nabla\eta_0\right) = \frac{\psi}{(d+\eta_0)^2}. \tag{4}$$

Eq. (4) is a nonlinear partial differential equation (PDE) and needs to be solved by numerical methods. Once the membrane deflection is determined using Eq. (4), the membrane tension can be obtained from Eq. (3). The reason for determining the static membrane tension of the membrane under magnetic force is to consider the static magnetic effect on the dynamic response of the membrane. The static magnetic effect is represented by the membrane tension in the dynamic equation of the membrane:

$$m\frac{\partial^2\eta}{\partial t^2} - \nabla\cdot[T_x\nabla(\eta_0+\eta)] + \frac{\psi}{(d+\eta_0+\eta)^2} + (P_+ - P_-) = 0, \tag{5}$$

where η is the vibration displacement of the membrane, and $(P_+ - P_-)$ is the acoustic pressure difference over the two sides of the membrane.

By substituting Eq. (1) into Eq. (5), one has

$$m\frac{\partial^2\eta}{\partial t^2} - \nabla\cdot[T_x\nabla(\eta)] - \frac{2\psi}{d^3}\eta + (P_+ - P_-) = 0. \tag{6}$$

As mentioned before, the membrane tension needs to be solved by numerical methods. As a first step, the membrane tension is approximated by a sine function expressed in Eq. (7). This approximation will later be validated by numerical results:

$$T_x = (T_o - T_m)\sin(\pi\xi) + T_m, \tag{7}$$

where $\xi = (x/L) + \frac{1}{2}$, and T_m is a constant which is directly proportional to the magnetic force. Substituting Eq. (7) into Eq. (6) yields

$$m\frac{\partial^2\eta}{\partial t^2} - \frac{(T_o - T_m)\pi}{L}\cos(\pi\xi)\frac{\partial\eta}{\partial x} - [(T_o - T_m)\sin(\pi\xi) + T_m]\frac{\partial^2\eta}{\partial x^2} - 2\frac{\psi}{d^3}\eta + (P_+ - P_-) = 0. \tag{8}$$

Using standard Galerkin procedure, η can be expanded as a series of in vacuo modes of the membrane with modal amplitude $\eta_{(r)}$:

$$\eta_{(r)}(t) = 2\int_0^1 \eta(x,t)\sin(r\pi\xi)\,\mathrm{d}\xi,\ \eta(x,t) = \sum_{r=1}^{\infty}\eta_{(r)}(t)\sin(r\pi\xi). \tag{9}$$

Hence, Eq. (8) can be rewritten as

$$\begin{aligned}&\left[-m\omega^2 + T_m\left(\frac{r\pi}{L}\right)^2 - 2\frac{\psi}{d^3}\right]\eta_{(r)} + 2\frac{(T_o - T_m)r\pi^2}{L^2}\\ &\quad\times\int_0^1\cos(\pi\xi)\sin(r\pi\xi)\eta\,\mathrm{d}\xi + 2(T_o - T_m)\left(\frac{r\pi}{L}\right)^2\int_0^1\sin(\pi\xi)\sin(r\pi\xi)\eta\,\mathrm{d}\xi\\ &\quad+ 2\int_0^1(P_+ - P_-)\sin(r\pi\xi)\,\mathrm{d}\xi = 0,\end{aligned} \tag{10}$$

where $r = 1, 2, 3, \ldots$.

As the coupling between the membrane and the acoustic pressure, (P_+–P_-), is too strong to be determined by the approach of room acoustics. It is reasonable to study the acoustic pressure by three parts. Part one is the upper surface pressure due to the harmonic incident wave, $P_i(x,t) = \exp[\mathrm{i}(\omega t - k_o x)]$, without considering the membrane vibration. Part two is the radiation acoustic pressure P_{rad} on the upper surface of the membrane. The third part is the acoustic back pressure from the cavity, denoted as P_b. Hence,

$$P_+ - P_- = (P_i + P_{\mathrm{rad}}) - (P_b). \tag{11}$$

P_{rad} can be calculated if the radiation impedance of the membrane is known. Let $Z^{(s)}_{\mathrm{rad},(r)}$ be the radiation impedance on the rth mode induced by the vibration of the sth mode. It can be calculated as [4]

$$Z^{(s)}_{\mathrm{rad},(r)} = L\sum_{n=0}^{\infty} c_n(2-\delta_{0n})I_2(n,s,r) \tag{12}$$

where c_n is the modal phase speed,

$$c_n = \frac{ic_o}{\sqrt{(n\pi c_o/\omega h)^2 + 1}}$$

and δ_{0n} is the Kronecker delta, I_2 is expressed as

$$I_2(n,s,r) = \begin{cases} \dfrac{nr\pi^2(\mathrm{e}^{\mathrm{i}n\pi} - \mathrm{e}^{-\mathrm{i}k_nL})(\mathrm{e}^{\mathrm{i}n\pi} + \mathrm{e}^{\mathrm{i}r\pi})}{[(k_nL)^2 - (n\pi)^2][(k_nL)^2 - (r\pi)^2]} \\ -\dfrac{\mathrm{i}k_nL\delta_{rn}}{(k_nL)^2 - (n\pi)^2}, & r \neq s \text{ and } k_oL/\pi \neq r \text{ or } s, \\ \dfrac{\mathrm{i}[1+(-1)^{r+s}]r\pi}{2[(k_oL)^2 - (r\pi)^2]}, & r \neq s \text{ and } k_oL/\pi = r \text{ or } s, \\ \dfrac{1}{4} - \dfrac{3\mathrm{i}}{4k_oL}, & r = s. \end{cases} \tag{13}$$

Similarly, the pressure inside the cavity can also be calculated via the radiation impedance, $Z^{(s)}_{b,(r)}$ involving two modes of the membrane. $Z^{(s)}_{b,(r)}$ can be calculated using the following expression [12,13]:

$$Z^{(s)}_{b,(r)} = -\rho_o\omega^2 \sum_{n=0}^{\infty} \frac{a^{(s)}_n a^{(r)}_n}{\mu_n} \cot(\mu_n d)(1+\delta_{0n}), \tag{14}$$

where $a^{(s)}_n$ and $a^{(r)}_n$ are the coupling coefficients defined as

$$a^{(q)}_n = \begin{cases} \int_0^1 \sin(q\pi\xi)\,\mathrm{d}\xi, & n = 0, \quad q = r \text{ or } s, \\ 2\int_0^1 \sin(q\pi\xi)\cos(n\pi\xi)\,\mathrm{d}\xi, & n > 0, \quad q = r \text{ or } s \end{cases} \tag{15}$$

and μ_n is calculated by

$$\mu_n = \sqrt{\left(\frac{\omega}{c_o}\right)^2 - \left(\frac{n\pi}{L}\right)^2}.$$

Eq. (10) becomes

$$\left[-m\omega^2 + T_m\left(\frac{r\pi}{L}\right)^2 - 2\frac{\psi}{d^3}\right]\eta_{(r)} + 2\frac{(T_o - T_m)r\pi^2}{L^2}\int_0^1 \cos(\pi\xi)\sin(r\pi\xi)\,\mathrm{d}\xi + 2(T_o - T_m)\left(\frac{r\pi}{L}\right)^2\int_0^1 \sin(\pi\xi)\sin(r\pi\xi)\eta\,\mathrm{d}\xi + K^{(s)}_{(r)}\eta^{(s)}_{(r)} = -P_{i,(r)}, \tag{16}$$

where $K_{(s)}^{(r)}$ is defined as cross acoustic stiffness with

$$K_{(r)}^{(s)} = \sum_{n=0}^{\infty}\left[\frac{\rho_o c_o L}{h^2} c_n(2-\delta_{0n}) I_2(n,s,r) + \rho_o \omega_c^2 \frac{a_n^{(s)} a_n^{(r)}}{\mu_n}\cot(\mu_n)(1+\delta_{0n})\right]. \tag{17}$$

By cosine Fourier analysis, we have

$$\sin(q\pi\xi) = \sum_{n=0}^{\infty} a_n^{(q)} \cos(n\pi\xi). \tag{18}$$

Since $\int_0^1 \cos(p\pi\xi)\cos(q\pi\xi)\,\mathrm{d}\xi = 0$ if p and q are integers, Eq. (16) becomes

$$\left[-m\omega^2 + T_m\left(\frac{r\pi}{L}\right)^2 - 2\frac{\psi}{d^3} + \frac{(T_o - T_m) r\pi^2}{L^2} a_1^{(r)}\right]\eta_{(r)} + (T_o - T_m)\left(\frac{r\pi}{L}\right)^2 \sum_{n=0}^{\infty} a_n^{(1)} a_n^{(r)} \eta_{(r)}(1+\delta_{0n}) + K_{(r)}^{(s)}\eta_{(r)}^{(s)} = -P_{i,(r)}. \tag{19}$$

Having found the cross acoustic stiffness, Eq. (19) can be cast as a truncated set of linear equations for the modal vibration amplitudes, $r = 1, 2, 3, \ldots, N$,

$$\begin{bmatrix} K_{(1)}^{(1)} + \kappa_{(1)} & K_{(1)}^{(2)} & \cdots & K_{(1)}^{(N)} \\ K_{(2)}^{(1)} & K_{(2)}^{(2)} + \kappa_{(2)} & \cdots & K_{(2)}^{(N)} \\ \cdots & \cdots & \cdots & \cdots \\ K_{(N)}^{(1)} & K_{(N)}^{(2)} & \cdots & K_{(2)}^{(N)} + \kappa_{(N)} \end{bmatrix} \begin{bmatrix} \eta_{(1)} \\ \eta_{(2)} \\ \cdots \\ \eta_{(N)} \end{bmatrix} = - \begin{bmatrix} P_{i,(1)} \\ P_{i,(2)} \\ \cdots \\ P_{i,(N)} \end{bmatrix}, \tag{20}$$

where

$$\kappa_N = -m\omega^2 + T_o\left(\frac{N\pi}{L}\right)^2 - \underbrace{2\frac{\psi}{d^3}}_{\text{Dynamic magnetic effect}} + \underbrace{(T_m)\left(\frac{N\pi}{L}\right)^2\left[1 - \sum_{n=0}^{\infty} a_n^{(1)} a_n^{(N)}(1+\delta_{0n})\right] + \frac{(T_o - T_m) N\pi^2}{L^2} a_1^{(N)}}_{\text{Static magnetic effect}}. \tag{21}$$

Eqs. (20) and (21) clearly show the magnetic effect on the vibration of the membrane type silencer. The third term and the last two terms on the right-hand side of Eq. (21) represent the dynamic magnetic effect and the static magnetic effect, respectively.

Therefore, if

$$2\frac{\psi}{d^3} > (T_m)\left(\frac{N\pi}{L}\right)^2\left[1 - \sum_{n=0}^{\infty} a_n^{(1)} a_n^{(N)}(1+\delta_{0n})\right] + \frac{(T_o - T_m) N\pi^2}{L^2} a_1^{(N)},$$

the dynamic magnetic effect will be able to over-rule the static effect on system stiffness. This would most likely happen at low frequencies. Otherwise, the system stiffness will increase, since the static effect is getting larger as N increases corresponding to higher frequencies. Moreover, Eq. (20) shows that the magnetic effect would only affect the direct cavity stiffness. It is because the magnetic effect only exists on the diagonal elements of the matrix in Eq. (20).

After solving Eq. (20) by standard matrix inversion techniques for $\eta_{(r)}$, the transmission loss provided by this silencer is calculated by

$$TL = -20\log_{10}\left|\frac{P_+}{P_i}\right| = -20\log_{10}\left|1 + \frac{P_{\mathrm{rad},x\to+\infty}}{P_i}\right| \tag{22}$$

with [4]

$$\frac{P_{\mathrm{rad}}}{P_i} = \mathrm{i}\omega\frac{L}{2}\sum_{r=1}^{\infty}\eta_r r\pi\,\mathrm{e}^{-\mathrm{i}k_o L/2}\left[\frac{\mathrm{e}^{\mathrm{i}(k_o L - r\pi)} - 1}{(k_o L)^2 - (r\pi)^2}\right]. \tag{23}$$

The influence of the magnetic effect on a typical drum-like silencer is now investigated. The configuration being used is the one optimized in Ref. [5] in the absence of magnetic force, with the following set of parameters:

$$L = 250\,\text{mm},\ d = 50\,\text{mm},\ T_o = 3611\,\text{N/m and } m = 0.01\,\text{kg/m}^2. \tag{24}$$

The stopband, defined as $TL > 10\,\text{dB}$, of this optimal drum-like silencer starts from frequency 390 Hz. This configuration is used here as a benchmark system.

For any given value of uniform magnetic forcing, ψ/d^2, Eqs. (3) and (4) can be used to find the distribution of the tension. The tension distribution is further approximated by a sine curve as given in Eq. (7). Fig. 2 illustrates how well the tension distribution is approximated by the sine curve for $\psi/d^2 = 809\,\text{Pa}$, a value which is shown later to yield a rather good transmission loss spectrum. More details of the tension calculation by the FE method are given in Ref. [14]. The trough of the sine curve, T_m, is 4740 Pa for this curve, and it is found to vary with ψ/d^2 roughly in a quadratic manner

$$T_m \approx 14.5094 + 0.9898\frac{\psi}{d^2} - 2.844 \times 10^{-4}\left(\frac{\psi}{d^2}\right)^2 \tag{25}$$

and the approximation is illustrated in Fig. 3.

The comparison in terms of the transmission loss spectra for a drum-like silencer without and with magnetic field is shown in Figs. 4(a) and (b), respectively. These two figures show an obvious shift of the transmission loss spectrum towards low frequencies due to the magnetic effect. When a static magnetic forcing of $\psi/d^2 = 809\,\text{Pa}$ is applied, peaks 'P1', 'P2' and 'P3' are shifted from 411, 725 and 942 to 325, 639 and 887 Hz, respectively. However, if the stopband level is defined as 10 dB, the stopband width is decreased from 671 to 455 Hz. This decreased stopband width is mainly due to a notable TL decrease at the trough 'T2'. Meanwhile, a slight increase in TL at 'T1' can also be observed. Given such a trade-off between the two troughs, and taking a liberal view of the stopband by ignoring the local violation of the rule of $TL > 10\,\text{dB}$ around 'T2', it may be said that the bandwidth hardly changes but merely shifts to lower frequencies.

It is shown for the drum-like silencer without magnetic forces that the response of the membrane is strong in the first two in vacuo modes. Detailed analysis reveals that the membrane deformation at the first peak is

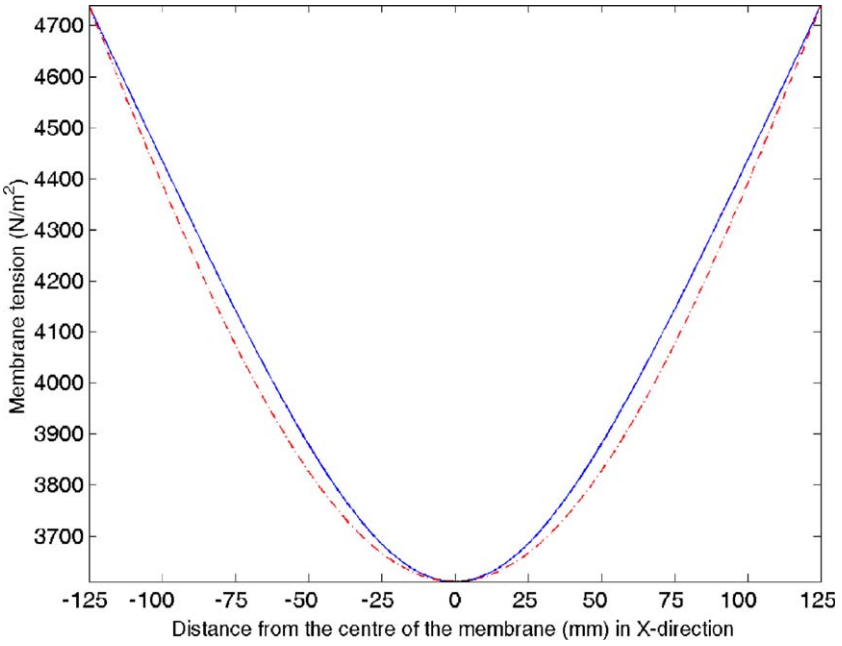

Fig. 2. Membrane tension caused by a uniform magnetic forcing of $\psi/d^2 = 809\,\text{Pa}$. The solid curve is obtained by the finite element computation and the dashed line is the approximation by a sine curve given in Eq. (7).

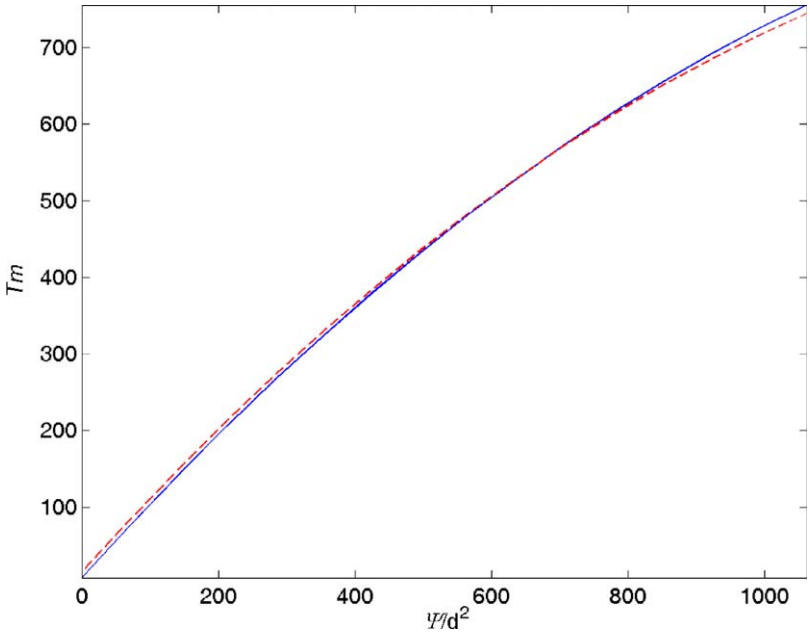

Fig. 3. Relationship between the static magnetic forcing ψ/d^2 and T_m, both with unit of Pascal. The solid line is the calculation result and the dashed line is the quadratic curve fitting given in Eq. (25).

actually very close to that of the second in vacuo mode, while the second peak to that of the first in vacuo mode. In other words, the cavity effect reversed the order of the in vacuo modes of the membrane, which is quite understandable. In fact, a shallow cavity will impose significant stiffness effect on the membrane mainly due to the air incompressibility [15,16]. The first in vacuo mode is significantly prohibited by the air motion inside the cavity, resulting in a significant shift to higher frequencies. This effect is, however, absent on the second in vacuo mode since the motion of the second in vacuo mode does not change the volume of the cavity. It is clear that controlling the frequency response of the first two modes is very important to ensure the effectiveness of the silencer. In practical implementation, however, the number of magnets inside is limited by the physical size of the cavity. Should too many magnets be put into the cavity, the cavity effect on the membrane will increase due to a reduction of the cavity volume. This is detrimental to the performance of the silencer at low frequencies. Therefore, it is important to optimize the placement of the magnets to promote the vibration of the first and the second modes of the membrane, while limiting the added stiffness effect of the cavity.

Actually, the low-frequency performance of this drum-like silencer can be enhanced by reducing the tension of the membrane, increasing the surface density of the membrane, or both without changing the geometry of the drum-like silencer. It has been shown, however, that these measures will also reduce the transmission loss level of the spectrum at the frequency 'T1' and consequently the bandwidth of the spectrum is dramatically reduced [4]. It is because the response of the membrane is mainly dominated by the cavity for the first mode, and by the structural properties for the second mode. The transmission loss level at the frequency 'T1' is caused by the intersection between the first and second modes. Reducing the tension of the membrane as mentioned before will enlarge the separation between the peaks 'P1' and 'P2', such reducing TL around the intersection area.

The theoretical analysis carried out above is based on the assumption that the magnetic force applied on the ferromagnetic membrane is uniform so that the membrane tension can be approximated by a cosine function. In order to provide a sufficiently high and uniform magnetic force on the ferromagnetic membrane, a very large magnet should be used. In the present case, the required static magnetic forcing is 809 Pa for a duct with a height of 50 mm and a ferromagnetic magnetic membrane with a thickness less than 0.05 mm. This can hardly be achieved using a single magnet. To tackle this problem, a pair of laminated rectangular magnets with alternative polar arrangement is employed to yield the required magnetic force. In total, three pairs of magnets are needed in the cavity to control the vibration of the membrane. Such arrangement helps yield

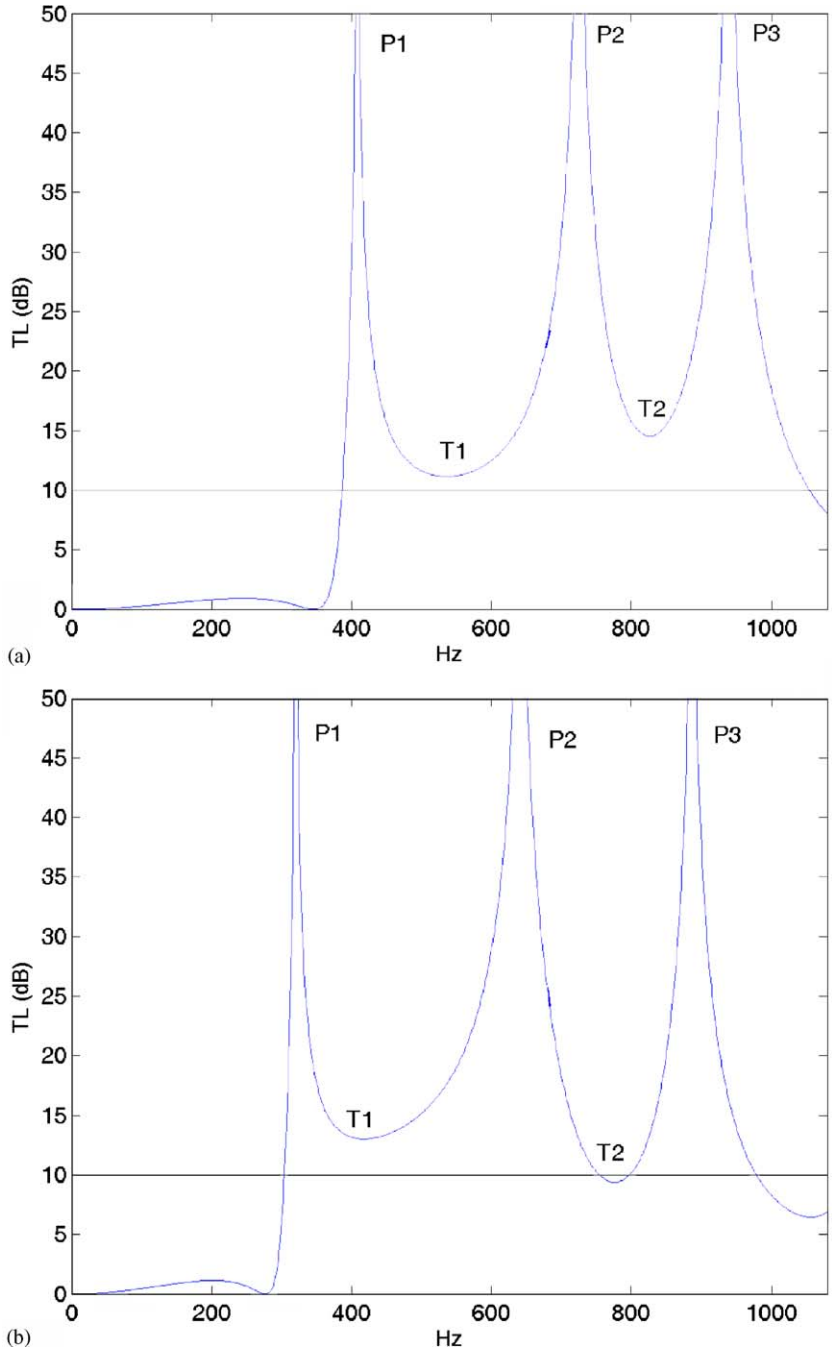

Fig. 4. Comparison of transmission loss spectra (a) without and (b) with magnetic forcing of $\psi/d^2 = 809\,\text{Pa}$. Other parameters are given in Eq. (24).

a strong enough magnetic force and reduce the space occupied by a large single magnet. The magnetic force applied on the membrane becomes, however, non-uniform. It is also observed that, using this arrangement, the static effect of the magnets is usually larger than the dynamic effect, which is detrimental to the performance of the silencer at low frequencies. To overcome this problem, a balancing cavity pressure is introduced inside the cavity to balance the static magnetic force applied on the membrane. The cavity pressure should be adjusted to minimize the static deflection of the membrane.

With all these measures, the magnetic force applied to the membrane is certainly non-uniform and the membrane tension is governed by a nonlinear differential equation (Eq. (4)). Although the 2D analysis carried out above gives a general understanding about the system, a more sophisticated model needs to be developed in order to optimize the performance of the silencer.

3. Finite element analysis

In order to predict the performance of the proposed silencer with multiple magnets and to optimize the design, an FE model is developed. This FE model considers the full coupling among the membrane vibration, acoustics pressure and the non-uniform magnetic field, and is experimentally validated. The FE model described in this section is coded in FemLab® and executed under the Matlab® environment. FemLab® is chosen to develop the program because of its open PDEs platform which allows the integration of multiphysics in a model like this.

The configuration under investigation is shown in Fig. 5 and the corresponding physical properties of the silencer are shown in Table 1. After the convergence test, the number of elements used is listed in Table 2. Key governing equations and the solution procedures are discussed in the following subsections.

3.1. Equations to be solved

The acoustic media inside the duct and cavity are modelled by Helmholtz equation using velocity potential, ϕ,

$$\nabla^2\phi + \left(\frac{\omega}{c_o}\right)^2 \phi = 0, \tag{26}$$

where ϕ, ω and c_o are velocity potential, angular frequency, and speed of sound, respectively. It should be noted that all variables defined in this section are dimensional rather than dimensionless.

The membrane response is modelled by an inhomogeneous Helmholtz equation with external force in terms of vibration displacement η,

$$\frac{\partial^2\eta}{\partial x^2} + \left(\frac{\omega}{c_m}\right)^2 \eta = \frac{F_m + p_d - p_c}{T}, \tag{27}$$

where

$$c_m = \sqrt{\frac{T}{m}} \tag{28}$$

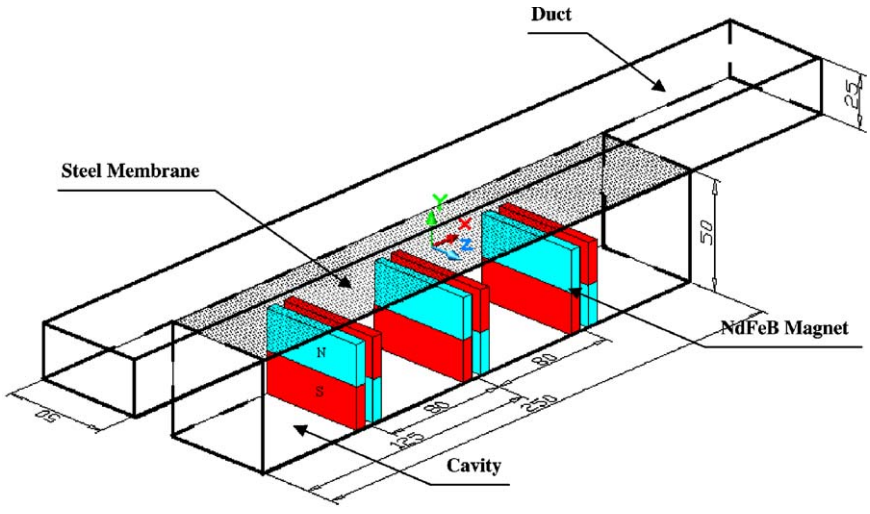

Fig. 5. Three-dimensional finite element model. Length unit (mm).

Table 1
Dimensions and material properties of the FE model

	Duct	Cavity
Length (mm)	400	250
Width (mm)	50	50
Height (mm)	25	50
	Magnet	Membrane
Dimensions (mm)	$50 \times 5 \times 35$	$250 \times 50 \times 0.05$
Magnetic flux density (H)	1.13	NA
Relative permeability	1.3	15
Young's module (GPa)	NA	196
Poisson's ratio	NA	0.25

Table 2
Type of element and no. of element of the FE model

Finite element model		Type of element	No. of element
Magnetic field		2D	79,273
Membrane deflection		1D	500
Acoustics	Duct	3D	809
	Cavity	3D	3164
	Membrane	2D	1660

in which T, m, F_m, p_d and p_c are the membrane tension, the membrane surface density, magnetic force, the duct pressure and the cavity pressures, respectively.

Maxwell's equations are used to describe the magnetic field distribution inside the cavity:

$$\nabla \times H = J,\ \nabla \cdot B = 0 \quad \text{and} \quad B = \mu(H + M) = \nabla \times A, \tag{29}$$

where B is the magnetic flux density, H the magnetic field intensity, J the current density, M the magnetic moment density vector of a specified source, μ the magnetic permeability of the membrane material and A the magnetic potential. The combination of the above equations gives

$$\nabla \times \left(\frac{1}{\mu}\nabla \times A - M\right) = J. \tag{30}$$

J is zero in the present case. Eq. (30) should be solved for finding A, which is further used to derive other variables defined in Eq. (29). According to Ref. [16], the magnetic force on the ferromagnetic membrane is

$$F_m = \frac{\mu(\mu_r - 1)}{2}[H^2(\tau/2) - H^2(-\tau/2)], \tag{31}$$

where μ_r is the relative permeability of the membrane and τ the thickness of the membrane.

For small deflection, the static deflection membrane can be described as

$$\frac{\partial}{\partial x}\left\{\left[\frac{E\tau}{2(1-v)}\left(\frac{\partial \eta_0}{\partial x}\right)^2 + T_o\right]\frac{\partial \eta_0}{\partial x}\right\} = F_m + 2F_m\eta_0 - P_{\text{gauge}}, \tag{32}$$

where η_0 is the static displacement of the membrane, E the Young's modulus, v the Poisson's ratio, T_o the applied pre-tension and P_{gauge} the cavity pressure. It is a highly nonlinear PDE. Once the static tension of the membrane is solved by FEA, the dynamic tension of the membrane T_x can be found by the

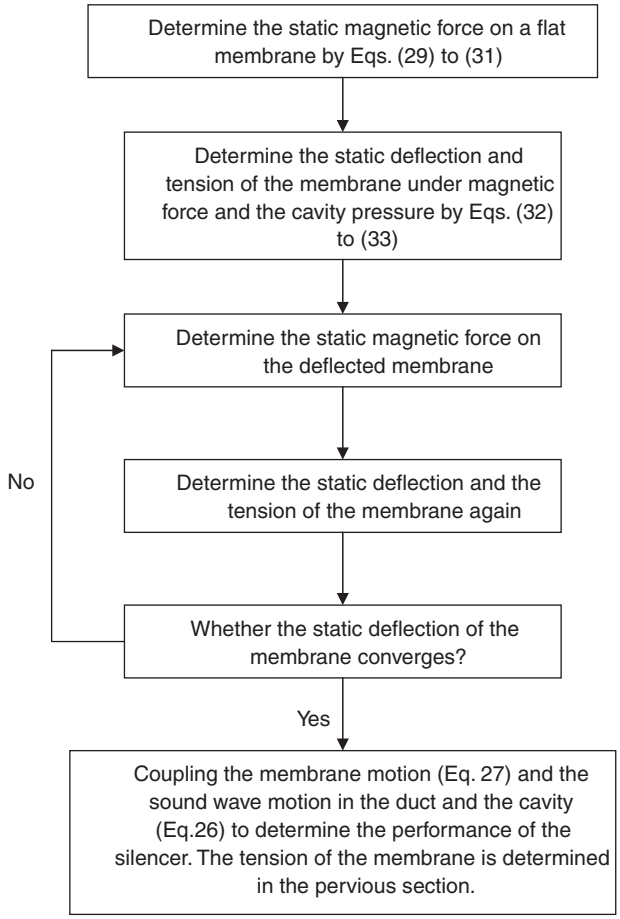

Fig. 6. Flow chart showing the procedure of the coupled FE analysis.

following equation:

$$T_x = \frac{Et}{2(1-v)}\left(\frac{\partial \eta_0}{\partial x}\right)^2 + T_o. \tag{33}$$

As the static magnetic force applied on the membrane and the deflection of the membrane are coupled, iteration is needed to determine the magnetic force and the deflection of the membrane. A flow chart showing the analysis procedure of the coupled FE analysis is given in Fig. 6.

3.2. Experimental validation

Experiments were carried out to verify the FE model. A schematic showing the experimental set-up is given in Fig. 7. The transmission loss spectrum was measured using the four-microphone, two-load method [6]. The function of each pair of microphones in upstream and downstream is to resolve the travelling wave and the reflected wave. The combination of two sets of linearly independent experiments eliminates the downstream reflection. By this method, the transmission loss can be measured even though there is a reflected wave at the downstream. A random noise signal was generated by a function generator. Two pairs of $\frac{1}{2}$ in microphones (B&K type 4187) were used together with a conditioning amplifier (B&K's Nexus 2691). The separation between each pair of microphones was 8 cm. As the distance from the two nearest microphones to the silencer was longer than the triple of the duct's height, the tube attenuation could not be neglected.

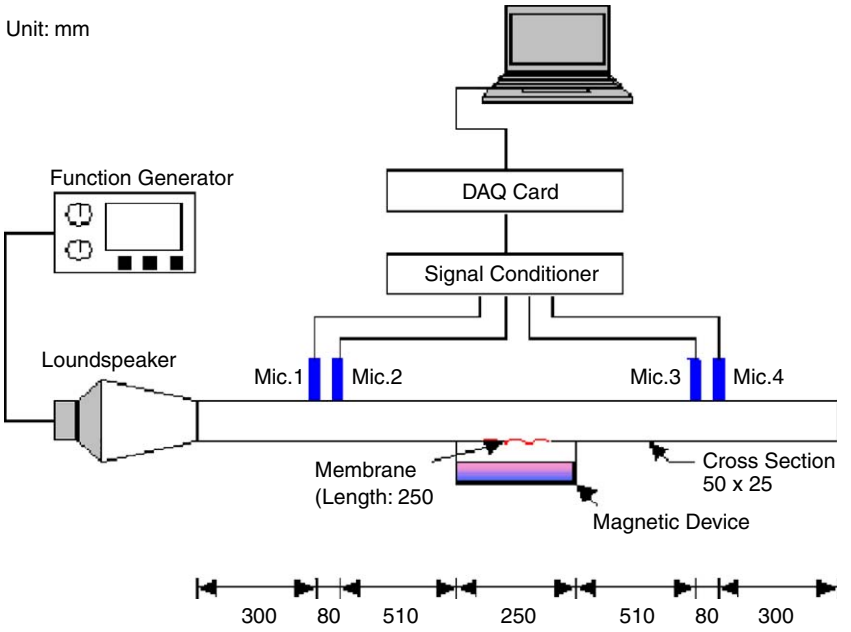

Fig. 7. Experimental set-up for the four-microphone, two-load measurement system. Length unit (mm). A function generator drives the loudspeaker for incident wave, and two pairs of microphones resolve the standing wave pattern in regions upstream and downstream of the membrane section of the duct. All signals are acquired simultaneously by a computer equipped with AD card.

Three pairs of magnets were placed at $\frac{1}{4}$, $\frac{1}{2}$ and $\frac{3}{4}$ length of the cavity. The lengths of the upstream and the downstream ducts are 1 m. The separation between the membrane and the magnets was adjusted by screws and springs which are shown in Fig. 8. By loosing or fastening the screws, the movable cylinders pushed the magnets towards or retreating from the cavity. The connection regions between the cylinders and the cavity were sealed by O-rings. The cavity pressure was supplied by a continuous air supply system and the cavity pressure was controlled by a pressure regulator. Signals from the four microphones were digitized by a DAQ card. The digital signal processing was carried out in Labview®. The initial membrane tension was measured by strain gauge which was connected to the stain gauge indicator (VISHAY P-3500). Fig. 9 shows a photo of the set-up.

When the separation between the membrane and the magnets is set at 2 mm, the predicted static magnetic force on the steel membrane is shown in Fig. 10. It can be seen that a maximum magnetic forcing of about 12300 Pa can be achieved at locations where magnets are placed.

According to Refs. [4,5], the optimal tension for the drum-like silencer without magnet is 2300 N. Therefore, the tension is kept at this value during the experiments. The variation of transmission loss spectrum with respect to the cavity pressure is shown in Fig. 11. Fig. 11(a) shows the theoretical prediction of the drum-like silencer without magnet and cavity pressure. Figs. 11(b)–(d) show the FE predictions (thick lines) and the experimental results (thin lines) for the same silencer geometry but with magnets and different cavity pressures. Fig. 11(a) shows that the stopband of the silencer without magnets and cavity pressure is $f \in [237, 370]$ Hz. With the deployment of the magnets and a cavity pressure of 1600 Pa, Fig. 11(b) clearly shows a shift of the effective region of the silencer towards lower frequencies. Numerical predictions using the FE model agree reasonably well with experiments apart from an obvious overestimation of the third peak. Although the low-frequency shift of the transmission loss spectrum can be achieved by using the magnetic force and a balancing cavity pressure, the overall transmission level is reduced as compared with Fig. 11(a). With a further increase of the cavity pressure to 1800 Pa, Fig. 11(c) still shows an acceptable agreement between the numerical prediction and measurement. However, this pressure increase results in an increase in the effective frequency region and a decrease in the overall transmission loss. This tendency is further enhanced when the cavity pressure is further increased to 1900 Pa. In this case, the FE model does not seem to be very accurate due to the fact that the static deflection of the membrane starts to be very large with the

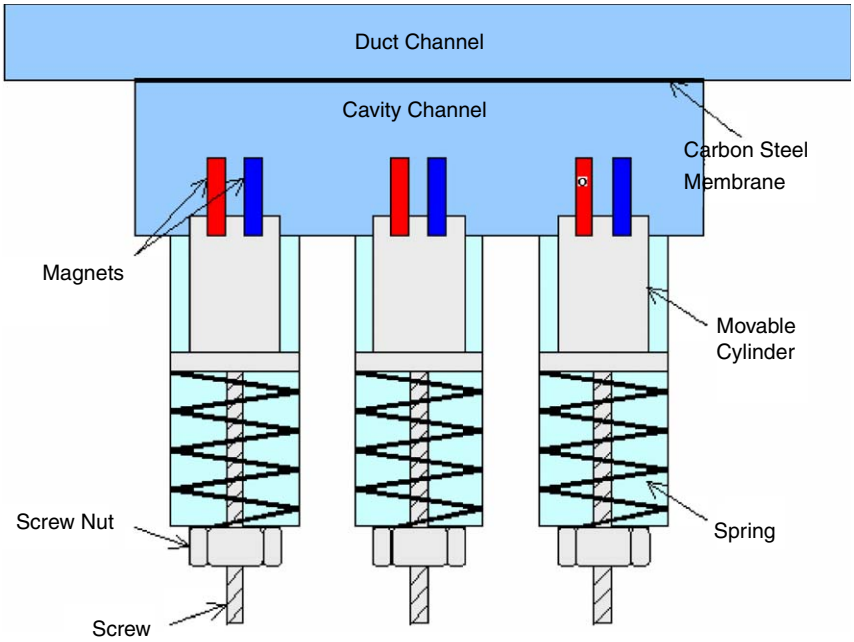

Fig. 8. A schematic design of the screws and springs mechanism which is used to control the separation between the magnets and the membrane.

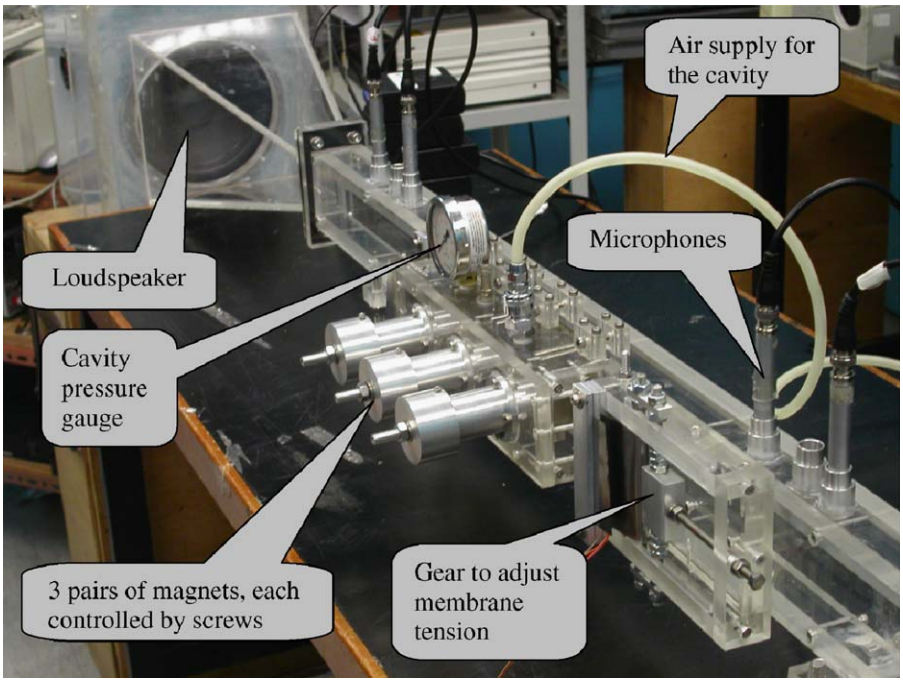

Fig. 9. A photo of the test rig.

increasing cavity pressure and the proposed FE model only applies to small deflection. Moreover, both simulations and experimental result indicate that the performance of the proposed silencer is very sensitive to the cavity pressure. The range of cavity pressure for achieving the low-frequency shift is quite narrow, which needs judicious tuning.

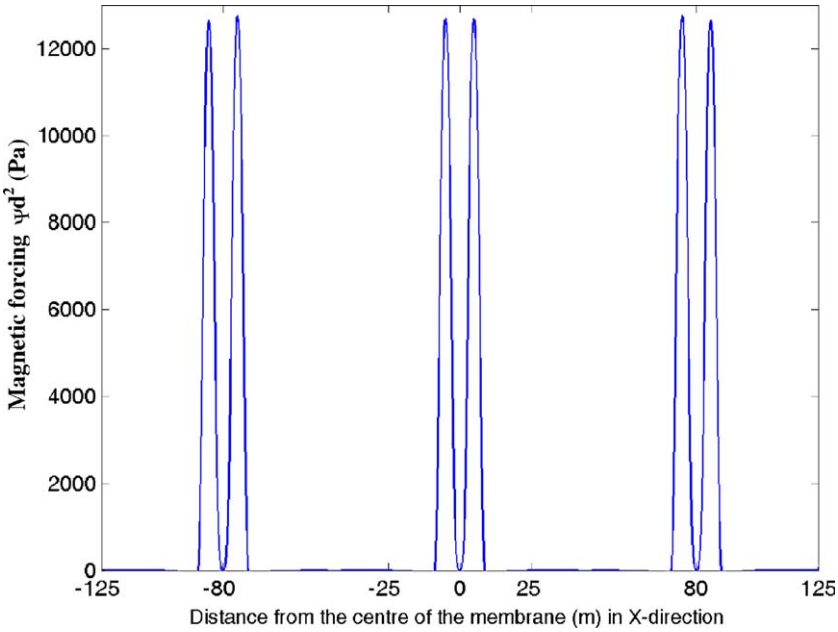

Fig. 10. Magnetic forcing distribution on a steel membrane using three pairs of laminated magnets.

3.3. *Region of static stability and the influence of the cavity pressure and initial tension*

The FE analysis predicted the best result can be obtained when the cavity pressure was 1350 Pa. This configuration, however, was not experimentally achieved. It was found that the membrane slammed into the magnets when the cavity pressure was less than 1400 Pa. This phenomenon is due to the instability of the ferromagnetic membrane under magnetic field. The situation is quite similar to putting a ferromagnetic body below a permanent magnet without any structural restoring forces. Although an equilibrium position can be found where the magnetic force balances the force of gravity, given small departures from that equilibrium point, the object either slams into the magnet or falls to the floor. In this case, the membrane tension serves as the structural restoring force to prevent the membrane from slamming into the magnets. This force increases when the cavity pressure decreases because a lower cavity pressure reduces the separation between the membrane and the magnet. Therefore, finding the minimum cavity pressure to maintain the stability of the membrane is crucial. The region of stability of the membrane under magnetic field can be found once the criteria of the small deflection of the membrane are defined.

Using the FE analysis, the region of stability of the membrane under magnetic field is obtained and shown in Fig. 12. In the figure, the solid line represents the separating line between the small deflection region and the large deflection region of the membrane. This line also represents the stability boundary of the membrane under magnetic effect. The points above this boundary keep the membrane in a stable situation, otherwise the membrane is unstable. This figure indeed shows that the membrane is unstable when the tension of the membrane is 2300 N with a cavity pressure of 1350 Pa. On the contrary, when the cavity pressures are 1600, 1800 and 1900 Pa, the three tested configurations all fall into the stable region (Marked as c1, c2 and c3 in Fig. 12, respectively).

Actually, Fig. 12 also shows that the region of static stability increases with the initial tension. This is understandable since increasing the initial tension enhances the restoring force on the membrane to prevent the static deflection of the membrane. This needs a lower cavity pressure to keep static balance of the membrane, but pushes the effective region of the silencer to higher frequencies.

Provided that the optimal configuration is defined by the lowest frequency of the first peak in the transmission loss spectrum, it can be seen that the best results of the drum-like silencer lay on the boundary of static stability curve for a given initial membrane tension. It is because the membrane deflection along the

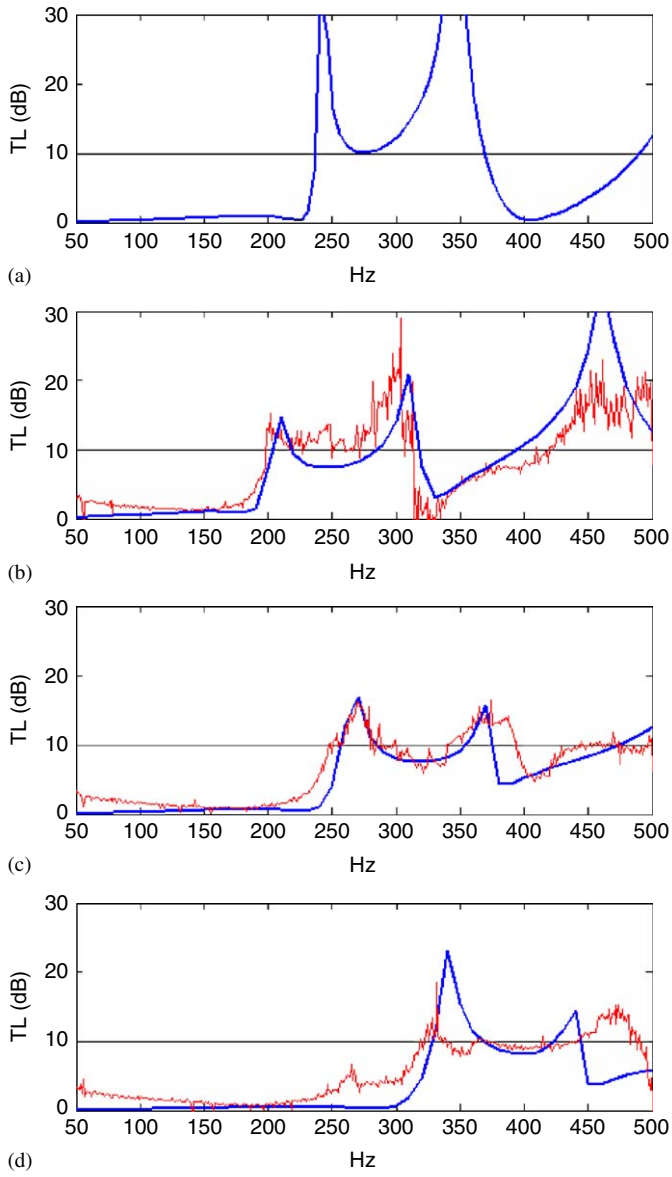

Fig. 11. Spectra of transmission loss for (a) the optimal drum-like silencer without magnets and cavity pressure; and the proposed silencer with cavity pressure of (b) 1600, (c) 1800 and (d) 1900 Pa. The experimental results (thin lines) and the predictions (thick lines) were obtained for the thin steel membrane under a tension of 2300 N.

boundary is maximized and hence the dynamic magnetic effect is also maximized. This phenomenon can be better seen in Fig. 13(a), in which the best performance for a proposed silencer with membrane tension of 1100 N can be achieved when the cavity pressure is 1710 Pa (corresponding to point a1 in Fig. 12). The frequency of the first peak in the spectrum retreats to 145 Hz. When the cavity pressure increases to 2050 Pa (corresponding to point a2 in Fig. 12), the lowest resonance frequency increases to 200 Hz. This observation suggests that the performance of the proposed silencer is very sensitive to the cavity pressure. A 20% increase in the cavity pressure leads to a 38% increase in the value of the frequency of the first peak in the transmission loss spectrum. When the cavity pressure is further increased to 2390 Pa, the frequency of the first peak of the spectrum is increased to 260 Hz. Along with the high-frequency shift of the spectrum when the cavity pressure increases, the overall transmission loss level is also increased. If the overall performance of the silencer is

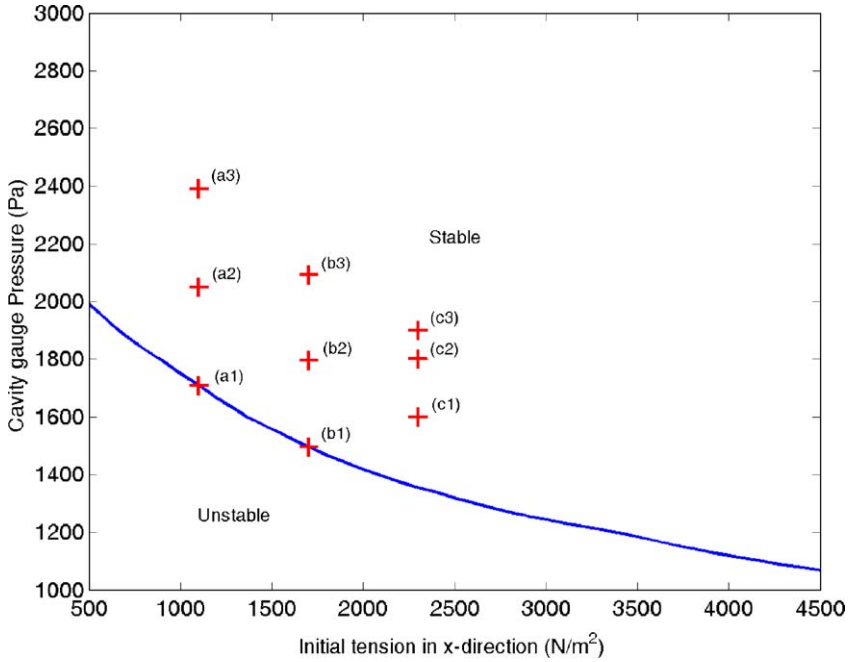

Fig. 12. Region of stability of a steel membrane under magnetic field. Points c1, c2 and c3 correspond to the parametric setting of Figs. 11(b)–(d), respectively. Points a1, a2, and a3 correspond to Fig. 13(a) and b1, b2, and b3 for Fig. 13(b).

assessed based on the transmission loss level at the first trough of the spectrum, the transmission loss levels are 3.5, 4.7 and 5.9 dB when the cavity pressures are 1710, 2050 and 2390 Pa, respectively.

In order to reveal the effect of the initial tension, Fig. 13(b) presents another group of comparisons when the initial tension of the membrane is maintained at 1700 N. Similar phenomenon as shown in Fig. 13(a) can be observed. However, this group of silencers is less sensitive to the cavity pressure and the increase in the overall transmission loss level due to the increase of the cavity pressure is less significant. In fact, Fig. 13(b) shows that the best performance can be achieved when the cavity pressure is 1500 Pa, for which the frequency of the first peak of the spectrum is 170 Hz with an overall transmission loss level of 6 dB. When the cavity pressure is increased to 1795 Pa, the first peak of the spectrum is increased to 205 Hz. In this case, the same 20% increase in the cavity pressure results in a 21% increase in the frequency of the first peak of the spectrum, to a less degree compared with the result shown in Fig. 13(a). When the cavity pressure is further increased to 2100 Pa, the first peak of the spectrum increases to 255 Hz.

Comparing the curves (a1) in Fig. 13 and (b1) in Fig. 13(b), it can be seen that while the spectrum is shifted to higher frequencies, the overall transmission level is increased when the membrane tension increases. The high-frequency shift of the spectrum is mainly due to the dominant increase of the structural stiffness caused by the increase of the tension over that of the magnetically induced stiffness. The reason for the overall transmission level increase with the initial tension can be explained by the theoretical analysis carried out in Section 2. In fact, the transmission loss level of the first trough of the spectrum is mainly affected by the separation between the first and second modes. A close proximity of the two modes helps maintain the transmission loss level of the first trough in the spectrum. Considering the characteristics of the first two modes discussed in Section 2, the dominant increase in the structural stiffness affects more the first mode than the second. This narrows down the separation between the first and second modes.

In summary, the optimal performance of the proposed silencer can be calculated when the criterion of the transmission loss level is defined. The cavity pressure and the initial tension of the membrane are two important parameters to be considered in the design of the silencer. Although the optimal combination of both lies along the boundary of the static stability curve, a compromise between the effective frequency range and the minimum *TL* level needs to be made in order to determine the individual value for each parameter. Upon defining the targeted *TL* level, minimum initial tension should be used to determine the appropriate cavity

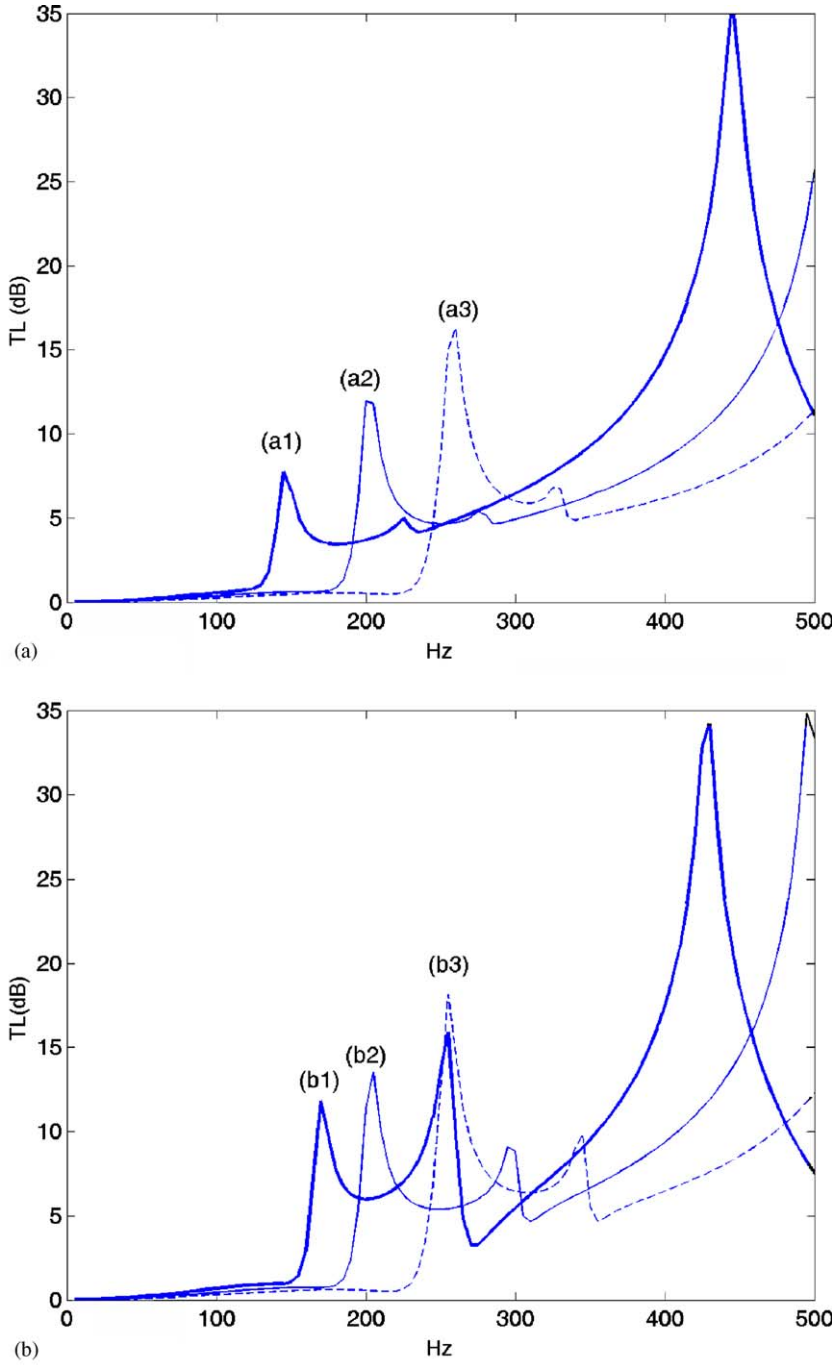

Fig. 13. TL spectra of proposed silencer under the initial tension of (a) 1100 N, and (b) 1700 N. In sub-figure (a), curves a1, a2, and a3 are for cavity gauge pressures of 1710, 2050, and 2390 Pa, respectively. In sub-figure (b), curves b1, b2, and b3 are for the cavity gauge pressures of 1500, 1795, and 2100 Pa, respectively.

pressure according to the stability curve to lower down the effective frequency range of the silencer. For comparison purposes, the $TL \geqslant 10$ dB criterion as defined in Ref. [17] is used here as an example. This criterion is defined as the range of frequency where the transmission loss is everywhere higher than the peak value of that in an expansion chamber which occupies three times as much cavity volume as does the proposed silencer.

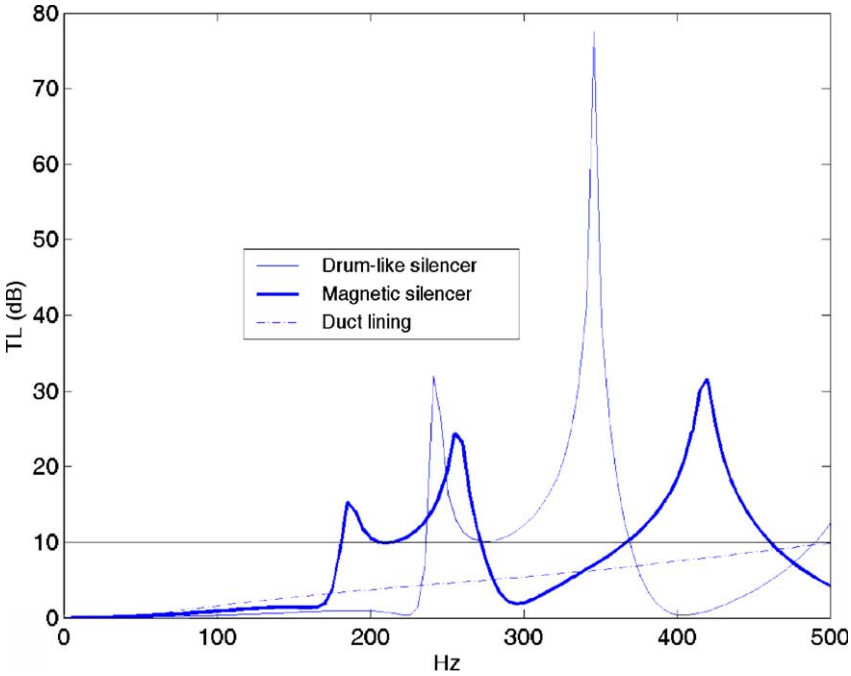

Fig. 14. Optimal *TL* spectra for the drum-like silencer (thin solid line), the proposed silencer (thick solid line), and duct lining by filling two cavities by glassfibre (dashed line).

When the cavity pressure is 1395 Pa, and the membrane tension is 2100 N, the optimal performance of the proposed silencer can be obtained and the result is shown in Fig. 14. The stopband of the proposed silencer is $f \in [181, 272]$ Hz. For benchmarking, the TL curves of the same drum-like silencer without magnet and cavity pressure and a traditional duct lining with the glassfibre falling in an equal volume expansion chamber are also shown in Fig. 14. For the latter, the flow-resistance of the glassfibre is 11.5 kN s/m^4. Comparing the three curves, it can be seen that the two drum-like silencers generally out-perform the duct lining chamber in low frequency region. The use of magnets and cavity pressure in the drum-like silencer significantly increases the *TL* between 170 and 225 Hz at the expense of higher frequency performance.

4. Conclusions

The feasibility of using magnetic force to enhance the low-frequency performance of drum-like silencers is explored using numerical and experimental means, leading to the following conclusions:

(1) The low-frequency performance of the drum-like silencer is mainly dominated by the first and the second in vacuo vibration modes of the membrane. Magnets should therefore be placed at appropriate locations to promote the responses of these two modes on one hand and to minimize the space occupied by the magnets and subsequently the cavity stiffness on the other.
(2) The magnetic effects are twofold: a dynamic effect and a static effect. The former introduces a magnetically-induced negative stiffness into the system, allowing a shift of the effective region of the silencer towards lower frequencies. The former effect, however, increases the tension of the membrane which tends to increase the natural frequency of the cavity backed membrane, which is detrimental to the low frequency performance of the silencer and needs to be suppressed. This can be done by controlling the static pressure inside the cavity.
(3) An FE model was developed and validated by experimental data. This model, considering the full coupling among the membrane vibration, the sound in fluid, and the magnetic field, provides a useful tool for

silencer design. The cavity pressure and the initial tension of the membrane are two important parameters to be considered. The optimal combination of both lies along the boundary of the static stability curve, and a compromise between the effective frequency range and the minimum *TL* level needs to be made in order to determine the individual value for each parameter.

(4) The performance of the silencer found to be very sensitive to the cavity pressure. The positioning of the magnets and the tuning of the cavity pressure turn out to be a delicate task in the practical implementation.

Appendix A

Assume that the tension on the membrane is a function of space, and express the vertical equilibrium of all forces acting on an element of area $\mathrm{d}x\,\mathrm{d}y$ (Fig. A1), the summation of the forces in the y direction yields

$$\left(T+\frac{\partial T}{\partial x}\,\mathrm{d}x\right)\left(\frac{\partial \eta_0}{\partial x}+\frac{\partial^2 \eta_0}{\partial x^2}\,\mathrm{d}x\right)\mathrm{d}y - T\,\frac{\partial \eta_0}{\partial x}\,\mathrm{d}y + \left(T+\frac{\partial T}{\partial y}\,\mathrm{d}y\right)\left(\frac{\partial \eta_0}{\partial y}+\frac{\partial^2 \eta_0}{\partial y^2}\,\mathrm{d}y\right)\mathrm{d}x - T\,\frac{\partial \eta_0}{\partial y}\,\mathrm{d}x + P_m(x,y)\,\mathrm{d}x\,\mathrm{d}y = 0, \tag{A.1}$$

which after neglecting small quantities of higher order, reduces to

$$T\frac{\partial^2 \eta_0}{\partial x^2}+\frac{\partial T}{\partial x}\left(\frac{\partial \eta_0}{\partial x}\right)+T\frac{\partial^2 \eta_0}{\partial y^2}+\frac{\partial T}{\partial y}\left(\frac{\partial \eta_0}{\partial y}\right)+P_m(x,y)=0. \tag{A.2}$$

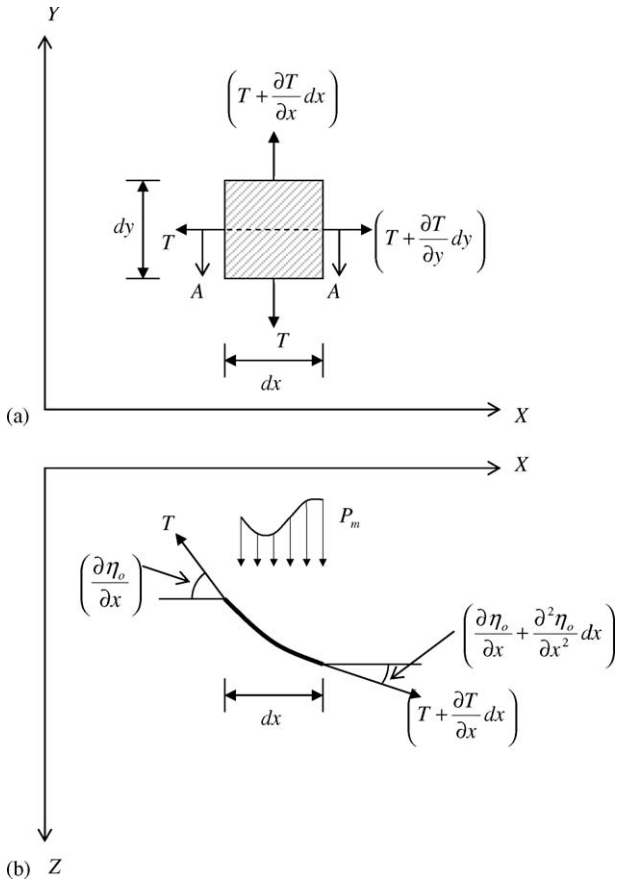

Fig. A1. Static forces equilibrium on an element: (a) plan view, (b) section view A-A.

Using the 2D Laplacian operator, Eq. (A.2) can be written as

$$\nabla \cdot (T \nabla \eta_0) = -P_m. \tag{A.3}$$

As the magnetic force per unit area on the membrane is defined as

$$P_m = -\frac{\psi}{(d+\eta_0)^2}, \tag{A.4}$$

where d is the separation between the ferromagnetic membrane and the magnet and Ψ is a constant magnetic function.

Therefore, Eq. (A.3) can be written as

$$\nabla \cdot (T \nabla \eta_0) = \frac{\psi}{(d+\eta_0)^2}. \tag{A.5}$$

References

[1] C.H. Hansen, S.D. Snyder, *Active Control of Noise and Vibration*, E & FN Spoon, 1997.

[2] T.M. Kostek, M.A. Franchek, Hybrid noise control in ducts, *Journal of Sound and Vibration* 237 (1) (2000) 81–100.

[3] J.M. De Bedout, M.A. Francher, R.J. Bernhard, L. Mongeau, Adaptive-passive noise control with self-tunning Helmholtz resonators, *Journal of Sound and Vibration* 202 (1) (1997) 109–123.

[4] L. Huang, A theoretical study of duct noise control by flexible panels, *Journal of the Acoustical Society of America* 106 (4) (1999) 1801–1809.

[5] L. Huang, Y.S. Choy, R.M.C. So, T.L. Chong, Experimental study of sound propagation in a flexible duct, *Journal of the Acoustical Society of America* 108 (2) (2000) 624–631.

[6] L. Huang, A theoretical study of passive control of duct noise using panels of vary compliance, *Journal of the Acoustical Society of America* 109 (6) (2001) 2805–2814.

[7] L. Huang, Modal analysis of a drum-like silencer, *Journal of the Acoustical Society of America* 112 (2002) 2014–2025.

[8] Y.S. Choy, L. Huang, Virbroacoustics of three dimensional drum silencer, *Journal of the Acoustical Society of America* 118 (4) (2002) 2313–2320.

[9] L. Huang, Y.S. Choy, Experimental studies of a drum-like silencer, *Journal of the Acoustical Society of America* 112 (2005) 2026–2035.

[10] L. Huang, A theory of reactive control of low-frequency duct noise, *Journal of Sound and Vibration* 238 (4) (2000) 575–594.

[11] A.D. Kerr, D.W. Coffin, On membrane and plate problems for which the linear theories are not admissible, *Journal of Applied Mechanics* (57) (1990) 128–133.

[12] A.J. Pretlove, Free vibrations of a rectangular panel backed by a closed rectangular cavity, *Journal of Sound and Vibration* 2 (3) (1965) 197–209.

[13] A.J. Pretlove, Forced vibration of a rectangular panel backed by a closed rectangular cavity, *Journal of Sound and Vibration* 3 (3) (1966) 252–261.

[14] Y.H. Chiu, L. Huang, L. Cheng, *The 32nd International Congress and Exposition on Noise Control Engineering, Control of Cavity Stiffness by Magnetic Forces*, 2003.

[15] L. Cheng, J. Nicolas, Radiation of sound into a circular cylindrical enclosure from point-driven plates with general boundary conditions, *Journal of the Acoustical Society of America* 91 (3) (1992) 1504–1513.

[16] L. Cheng, Y.Y. Li, J.X. Gao, Energy transmission in a mechanically-linked double-wall structure coupled to an acoustic enclosure, *Journal of the Acoustical Society of America* 117 (5) (2005) 2742–2751.

[17] L. Huang, Parametric study of a drum-like silencer, *Journal of Sound and Vibration* 269 (2004) 467–488.